Self-organization in an excitable reaction-diffusion system. III. Motionless localized versus propagating-pulse solutions

Aya Ito and Takao Ohta

Department of Physics, Ochanomizu University, Tokyo 112, Japan
(Received 14 February 1992)

In a series of papers, we have studied pattern dynamics in the Bonhoeffer–van der Pol type reaction-diffusion system which is a coupled set of equations for an activator and an inhibitor and exhibits excitability. We have been concerned mainly with localized motionless solutions in one dimension, which have been shown to be stable when the diffusion constant of the inhibitor is sufficiently large. In this paper, we shall explore how the properties of the system change when we decrease the diffusion constant. It is shown that a motionless localized solution turns out to be unstable in such a situation while a propagating-pulse solution can exist stably. This crossover from the motionless to the pulse solutions does not occur as a clear bifurcation. There is a parameter regime where the two solutions can coexist, and rich variety of dynamical patterns is expected.

PACS number(s): 05.70.Ln, 82.20.Mj, 87.10.+e

I. INTRODUCTION

The characteristic features of nonequilibrium open systems are temporal order and existence of a stable spatially localized pattern. The former is well known and has been discussed in many papers. On the other hand, the relevancy of the latter, especially a *motionless* localized pattern, has not been paid much attention except for a few theoretical studies [1–3]. Experimentally, however, such localized (periodic) patterns have recently been observed in several systems [4–8] far from equilibrium.

In this series of papers [9,10] which will be referred to as I and II, respectively, we have investigated the stability of spatially localized pattern (domain) and the oscillatory motion of the domains based on the Bonhoeffer–van der Pol (BvP) type model equation in one dimension. The model consists of a coupled set of reaction-diffusion equations for the activator u and the inhibitor v and reads

$$\epsilon \tau \partial_t u = \epsilon^2 \partial_x^2 u + f(u) - v , \tag{1.1a}$$

$$\partial_t v = \epsilon D \partial_x^2 v + \beta u - \gamma v , \tag{1.1b}$$

where all the parameters ϵ, τ, D, β, and γ are assumed to be positive. Note that the definition of the diffusion constant for v is different from that in I and II. The function $f(u)$ has a cubiclike nonlinearity such that $f(u) = u(1-u)(u-a)$ with a constant. To make the calculation tractable, we often utilize the piecewise linear form of $f(u)$ [11], i.e.,

$$f(u) = -u + \Theta(u - a) , \tag{1.2}$$

where $\Theta(x)$ is the Heaviside step function. When $\epsilon \ll D$, Eqs. (1.1) admit a spatially localized motionless solution. The spatial variation of the solution is depicted in Fig. 1 below in Sec. II. We call the region where u is positive (strictly speaking, the region $u > a$) an excited domain while the region where u is negative a rest domain. The domain boundary is called an interface.

In the first paper [9], we studied, by a singular perturbation method [12], the Hopf bifurcation of spatially periodic excited domains, which occurs when the parameter τ is decreased. What we have found is that when the width of the excited domain is neither extremely small nor comparable to the spatial period, the periodic domains undergo an in-phase oscillation for τ smaller than the critical value τ_c.

In the second paper [10], we have derived the phase-amplitude equation to study the dynamical order of interacting oscillating domains behavior at postthreshold.

All these studies are restricted to the case $\epsilon \ll D$. In this paper, we shall investigate the property of Eqs. (1.1) by changing the ratio ϵ / D. As is well known, Eqs. (1.1) reduce to the FitzHugh-Nagumo equation [13] in the limit $D \to 0$ (and $\gamma = 0$) where a propagating-pulse solution can exist stably. Thus our primary concern is how the crossover from a motionless localized solution for $\epsilon \ll D$ to a propagating-pulse solution for $\epsilon \gg D$ occurs. To our knowledge such a phenomenon has neither been studied theoretically nor been observed experimentally. However, it is expected that the crossover by changing D might play an important role for information transportation in some biological systems. Computer simulations of Eqs. (1.1) have indeed demonstrated breakup of a motionless domain into two pulses propagating to the opposite directions [14]. It is remarked here that the singular perturbation method which assumes $\epsilon \ll D$ cannot be used in the present analysis.

Organization of the paper is as follows. In the next section, we obtain a motionless localized solution by using the piecewise linear dynamics (1.2). In Sec. III, on the other hand, we derive a propagating-pulse solution. We focus our attention on the effect of the diffusion of the inhibitor. In Sec. IV, we compare the profiles of the motionless and propagating solutions by changing the parameters D and a. In Sec. V, we make some concluding remarks. The details to derive the pulse solution in Sec. III are summarized in the Appendix.

II. MOTIONLESS LOCALIZED SOLUTION

A motionless localized solution of BvP equation has been investigated by Koga and Kuramoto [1]. In this section, we extend their results and show that the system does not possess a stable motionless solution as the diffusion constant D becomes small.

Without loss of generality, we may assume that the steady nonuniform solution of Eqs. (1.1) is symmetric with respect to $x=0$, and that the excited region is confined to the interval $-R<x<R$. The steady solution is denoted by $u(x,t)=u_s(x)$ and $v(x,t)=v_s(x)$. From Eqs. (1.1) with the piecewise linear form of $f(u)$ given by Eq. (1.2) and with $\partial_t u_s=\partial_t v_s=0$, we can eliminate u_s so that Eq. (1.1b) becomes the following differential equation for v_s:

$$\epsilon^3 D v_s'''' - \epsilon(\epsilon\gamma+D)v_s''+\beta+\gamma=0 , \qquad (2.1)$$

where a prime indicates the derivative with respect to the argument. Since Eq. (2.1) is linear in v_s, the solutions u_s and v_s can be obtained as a linear combination of the exponentials $\exp(\alpha_i x)$, where α_i are zeros of the polynomial

$$P(\alpha)=\alpha^4-\frac{\epsilon\gamma+D}{\epsilon^2 D}\alpha^2+\frac{\beta+\gamma}{\epsilon^3 D} . \qquad (2.2)$$

Equation $P(\alpha)=0$ has four roots α_1, α_2, $-\alpha_2$, and $-\alpha_1$ ($\alpha_1>\alpha_2>0$ or $\alpha_1=\alpha_2^{c.c.}$. Superscript c.c. indicates complex conjugate.) Koga and Kuramoto [1] assumed that these are real, but here we allow that the roots may be complex.

The coefficients of the exponentials are determined by the boundary conditions, $u_s=v_s=0$ at $x=\pm\infty$, and the matching conditions of u_s and v_s and their first derivatives at $x=\pm R$. After a straightforward calculation the motionless localized solution is obtained as

$$u_s(x)=\begin{cases} A_{12}e^{-\alpha_1 R}\cosh\alpha_1 x+A_{21}e^{-\alpha_2 R}\cosh\alpha_2 x+\dfrac{\gamma}{\beta+\gamma} & \text{for } 0<|x|<R \\[2mm] -A_{12}e^{-\alpha_1|x|}\sinh\alpha_1 R-A_{21}e^{-\alpha_2|x|}\sinh\alpha_2 R & \text{for } R<|x| , \end{cases} \qquad (2.3a)$$

$$v_s(x)=\left[\epsilon^2\frac{d^2}{d^2 x}-1\right]u_s(x)+\Theta(R-|x|)$$

$$=\begin{cases} B_{12}e^{-\alpha_1 R}\cosh\alpha_1 x+B_{21}e^{-\alpha_2 R}\cosh\alpha_2 x+\dfrac{\beta}{\beta+\gamma} & \text{for } 0<|x|<R \\[2mm] -B_{12}e^{-\alpha_1|x|}\sinh\alpha_1 R-B_{21}e^{-\alpha_2|x|}\sinh\alpha_2 R & \text{for } R<|x| , \end{cases} \qquad (2.3b)$$

where

$$A_{\mu\nu}=\frac{\gamma-\epsilon D\alpha_\mu^2}{\epsilon^3 D\alpha_\mu^2(\alpha_\mu^2-\alpha_\nu^2)} , \qquad (2.4a)$$

$$B_{\mu\nu}=(\epsilon^2\alpha_\mu 2-1)A_{\mu\nu} , \quad \mu,\nu=1,2 . \qquad (2.4b)$$

Here the half-width R of the excited region is determined by the relation

$$u_s(\pm R)=a . \qquad (2.5)$$

Equation (2.5) is the definition of location of the domain boundary and specifies the a dependence of R.

Figure 1 is an example of the motionless localized solution expressed by Eqs. (2.3). Figures 2 and 3 show the relation between the parameter a and the width R graphically for several values of the diffusion constant D of the inhibitor. Other parameters are chosen as $\epsilon=0.1$, $\gamma=\frac{1}{3}$,
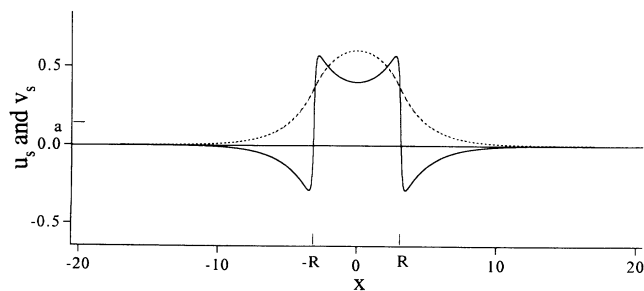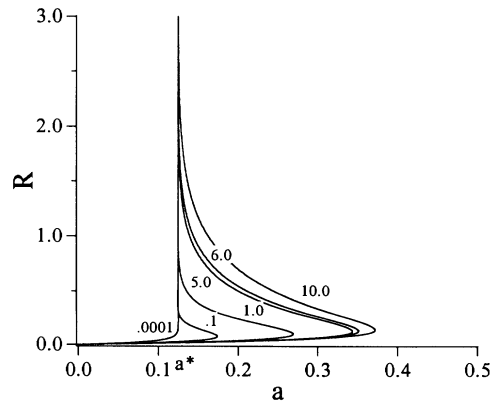

FIG. 1. Profile of the motionless localized solution u_s (solid line) and v_s (dashed line) for $\epsilon=0.1$, $D=50.0$, $\gamma=\frac{1}{3}$, $\beta=1.0$, and $a=0.14$. The width R is given by $R=4.404$.

FIG. 2. Domain width R as a function of a for $\gamma=\frac{1}{3}$ and for $\epsilon=0.1$ and $\beta=1.0$. The digits on each curve indicate the value of D.
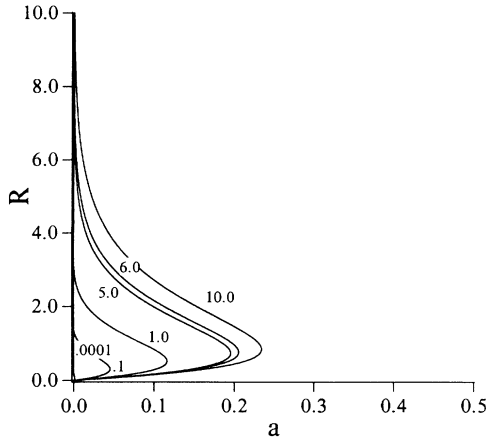
FIG. 3. Domain width R as a function of a for $\gamma = 0$ and $\epsilon = 1$. Other parameters are the same as those in Fig. 2.

$\beta = 1$ in Fig. 2, and as $\epsilon = \beta = 1$, $\gamma = 0$ in Fig. 3. In Fig. 2 it is found that when D is large enough (for example, $D = 1.0$), two steady solutions with $R = R_1$ and R_2 ($R_1 > R_2$) exist for some range of a. Koga and Kuramoto [1] have shown that the R_2 branch is always unstable, while the R_1 branch is stable. Note that the R_1 branch is in the region $a > \gamma / [2(\beta + \gamma)] \equiv a^*$, where the rest state

is more stable than the excited state. If $a = a^*$, the rest and the excited states are equally stable. Thus when the parameter a approaches a^* from above the width R_1 becomes infinite. Notice that when D is small enough (for example, $D = 0.0001$) no solution exists in the region $a > a^*$, so that a motionless localized stable solution does not exist.

A simpler case where $\gamma = 0$ is shown in Fig. 3. Since $a^* = 0$ in this case, the R_1 branch exists always for finite values of D, although the value of R_1 becomes extremely small for $D \to 0$.

III. PULSE SOLUTION

In this section we shall derive a solitary pulse solution of the BvP equation which includes, as a special case, a pulse solution of the FitzHugh-Nagumo equation [13]. We seek a propagating-pulse solution of Eqs. (1.1) with Eq. (1.2), which travels to the right with a propagating velocity c. The pulse solution is denoted by $u(x,t) = u_c(z)$ and $v(x,t) = v_c(z)$, with $z = x - ct$. Here the excited region is confined to $0 < z < z_1$, where the boundaries $z = 0$ and $z = z_1$ are defined by the conditions (3.6) below.

First we solve the differential equation of v_c, which is given from Eqs. (1.1) by

$$\epsilon^3 D \frac{d^4 v_c}{dz^4} + \epsilon^2 c(\tau D + 1) \frac{d^3 v_c}{dz^3} + \epsilon(\tau c^2 - \epsilon\gamma - D) \frac{d^2 v_c}{dz^2} - c(\epsilon\gamma\tau + 1) \frac{dv_c}{dz} + (\beta + \gamma)v_c - \beta\Theta(z)\Theta(-z + z_1) = 0 . \tag{3.1}$$

Details to obtain the solution are given in the Appendix. Here we write the final result.

$$u_c(z) = \begin{cases} A_{11} e^{\alpha_1 z} + A_{12} e^{\alpha_2 z} & \text{for } z > 0 \\ A_{21} e^{\alpha_1 z} + A_{22} e^{\alpha_2 z} + A_{23} e^{\alpha_3 z} + A_{24} e^{\alpha_4 z} + \dfrac{\gamma}{\beta + \gamma} & \text{for } 0 < z < z_1 \\ A_{33} e^{\alpha_3 z} + A_{34} e^{\alpha_4 z} & \text{for } z_1 < z , \end{cases} \tag{3.2a}$$

$$v_c(z) = \begin{cases} B_{11} e^{\alpha_1 z} + B_{12} e^{\alpha_2 z} & \text{for } z > 0 \\ B_{21} e^{\alpha_1 z} + B_{22} e^{\alpha_2 z} + B_{23} e^{\alpha_3 z} + B_{24} e^{\alpha_4 z} + \dfrac{\beta}{\beta + \gamma} & \text{for } 0 < z < z_1 \\ B_{33} e^{\alpha_3 z} + B_{34} e^{\alpha_4 z} & \text{for } z_1 < z , \end{cases} \tag{3.2b}$$

where α_1, α_2, α_3, and α_4 are the zeros of the polynomial

$$P(\alpha) = \alpha^4 + \frac{c(\tau D + 1)}{\epsilon D} \alpha^3 + \frac{\tau c^2 - \epsilon\gamma - D}{\epsilon^2 D} \alpha^2 - \frac{c(\epsilon\gamma\tau + 1)}{\epsilon^3 D} \alpha + \frac{\beta + \gamma}{\epsilon^3 D} . \tag{3.3}$$

Notice that signs of all the coefficients except for that of the α^2 term are definite. Especially only the coefficient of the linear term is negative. Hence we may put, without loss of generality,

$$\text{Re}(\alpha_1) \geq \text{Re}(\alpha_2) > 0 > \text{Re}(\alpha_3) \geq \text{Re}(\alpha_4) , \tag{3.4}$$

where $\text{Re}(\alpha_i)$ stands for the real part of α_i.

The coefficients A_{ij} and B_{ij} are determined by the boundary conditions and the matching conditions at the domain boundaries which are the same as those given in Sec. II. A_{ij} and B_{ij} depend on the velocity c and the pulse width z_1 as given in the Appendix. These two unknown quantities should be determined by the relations

$$a = A_{11} + A_{12} , \tag{3.5a}$$

$$a = A_{33} e^{\alpha_3 z_1} + A_{34} e^{\alpha_4 z_1} . \tag{3.5b}$$

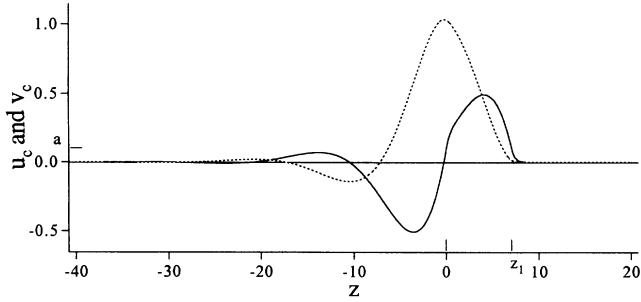Equations (3.5) come from the definition of the location

FIG. 4. Profile of the solitary pulse solution u_c (solid line) and v_c (dashed line) for $\epsilon=\tau=\beta=D=1$, $a=0.1002$, and $\gamma=0$. The width z_1 and the velocity c are given by $z_1=7.052$ and $c=2.56$.

of domain boundaries

$$u_c(0)=u_c(z_1)=a \ . \tag{3.6}$$

Figure 4 is an example for the pulse solution of the BvP equation given by Eqs. (3.2). Figures 5 and 6 show the a dependence of c and the relation between c and z_1, respectively. These are obtained by solving (3.5) simultaneously, for fixed values of D. Here we have put $\epsilon=\tau=1$ and $\gamma=0$, because this choice of the parameters is convenient when we compare the pulse solution obtained here and that of FitzHugh-Nagumo equation obtained by Rinzel and Keller [15]. They have expressed the relation between the parameter a and the propagating velocity c graphically as in Fig. 5, and have found that there is a regime for a, where two pulse solutions can exist. Furthermore, they have shown by a linear stability analysis that the slower and narrower solution is always unstable, while the faster and wider solution is stable.

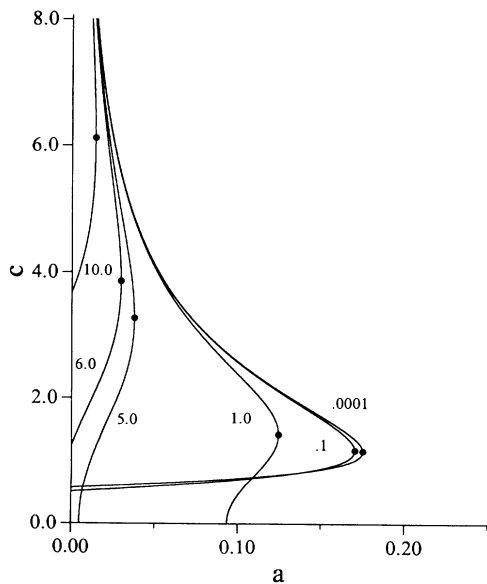It is remarked here that when both D and a are very

FIG. 5. Pulse speed c as a function of a. The digits on each curve indicate the value of D. The dots show the maximum point $a=a_c$ of each curve.
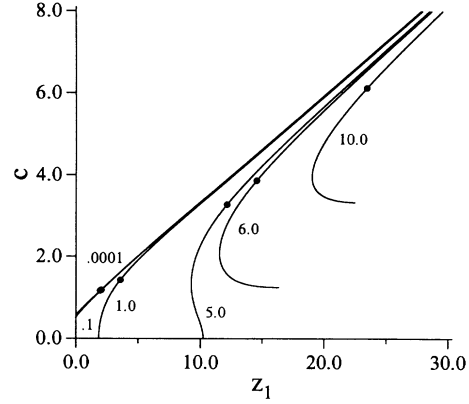

FIG. 6. Relation between the pulse speed c and the width z_1. The digits on each curve indicate the value of D. The dots show the values of c and z_1 at $a=a_c$ in Fig. 5.

small, we have to take account of another solution. That is, a traveling wave train turns out to be more stable than an isolated propagating pulse. This will be discussed in the next section.

We have confirmed that the profile of the pulse solution as well as the a-c relation of the BvP equation for $D=0.0001$ and 0.1 almost agree with that for obtained by Rinzel and Keller [15]. It is found from Fig. 5, however, that depending on the magnitude of the diffusion constant D, the a-c relation changes drastically. When it is extremely small, or larger than 6.0, the smaller velocity c attains a finite value in the limit $a\rightarrow0$. For intermediate values of D, however, the slower branch terminates at a finite value of a.

Figure 6 displays the relation between c and the pulse width z_1. The dot on each curve corresponds to that in Fig. 5. It is noticed that the velocity c above the dot is almost linear in z_1. When the diffusion constant D is increased with c fixed, the width z_1 increases. This is expected since, when D is large, the pulse width has to be large otherwise it is eliminated by the inhibitor. Furthermore, we see that the velocity c and the width z_1 do not depend substantially on the diffusion constant D, as both c and z_1 become larger. This is again expected since, when the velocity is large enough, the diffusion does not play any decisive role in the extension of v.

In order to understand the c-z_1 relation for small values of c obtained in Fig. 6, we solve approximately the following equation:

$$A_{11}+A_{12}=A_{33}e^{\alpha_3 z_1}+A_{34}e^{\alpha_4 z_1} \ . \tag{3.7}$$

This is obtained by equating (3.5a) and (3.5b). First we need to evaluate α_i ($i=1,2,3,4$). Let us introduce the scaled quantities

$$\hat{D}=D\tau, \quad \hat{a}=a\epsilon, \quad \hat{c}=c\tau, \quad \hat{\gamma}=\gamma\tau\epsilon, \quad \hat{\beta}=\beta\tau\epsilon \ . \tag{3.8}$$

Equation $P(\alpha)=0$ with $P(\alpha)$ given by (3.3) can be written as

$$\hat{D}\hat{\alpha}^4+\hat{c}(\hat{D}+1)\hat{\alpha}^3+(\hat{c}^2-\hat{\gamma}-\hat{D})\hat{\alpha}^2-\hat{c}(\hat{\gamma}+1)\hat{\alpha}+\hat{\beta}+\hat{\gamma}$$
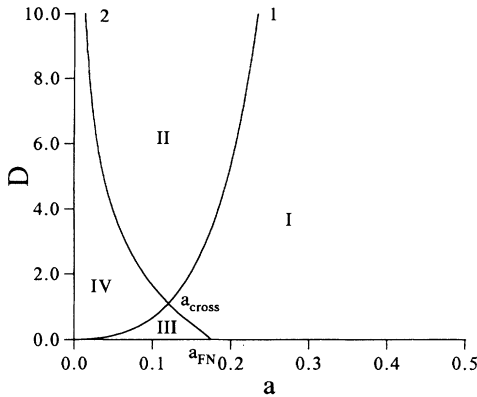$$=0 \ . \tag{3.9}$$

FIG. 7. Phase diagram in the a-D plane for motionless and pulse solutions. On the left side of the line 1 (2), a motionless (pulse) solution exists.

FIG. 8. The values of a and D for motionless domains shown in Fig. 9.

Hereafter we omit the caret in this section. For simplicity, we consider the case $\beta=1$ and $\gamma=0$. We solve Eq. (3.9) for a large D expansion. In this limit the solutions are found to be real. The lowest-order solution is given by

$$\alpha_2=\alpha_3=0, \quad \alpha_i^2+c\alpha_i-1=0 \quad (i=1,4) . \tag{3.10}$$

We may expand α in powers of $1/D$. However, the expansion should be in terms of $D^{-1/2}$ for α_2 and α_3. After some elementary calculations we obtain

$$\alpha_2=-\alpha_3=D^{-1/2}+(1+c^2)D^{-3/2}+O(D^{-2}) . \tag{3.11}$$

The $1/D$ term is absent because of $\beta=1$. On the other hand, it is convenient to express α_1 and α_4 in the follow-
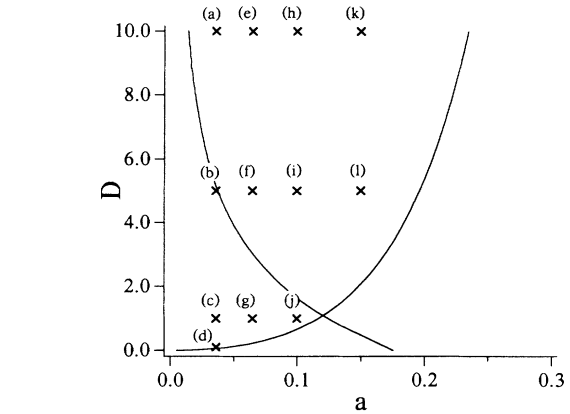
ing combinations up to order $1/D$:

$$\alpha_1+\alpha_4=-c-c/D , \tag{3.12a}$$

$$\alpha_1\alpha_4=-1+(1+c^2)/D . \tag{3.12b}$$

Each term in Eq. (3.7) contains a factor $1-\exp(-\alpha_i z_1)$. The above result implies that we may replace it by 1 for $i=1$ and 4 provided that z_1 becomes large as D is increased. This is indeed the case for small values of c as shown in Fig. 6. Substituting (3.11) and (3.12) into (3.7) and using the above fact, we obtain in the limit $c\rightarrow0$

$$\frac{1}{4\sqrt{D}}\left[1+\frac{3}{D}+O(D^{-2})\right]=1-\exp(-z_1 D^{-1/2}) . \tag{3.13}$$

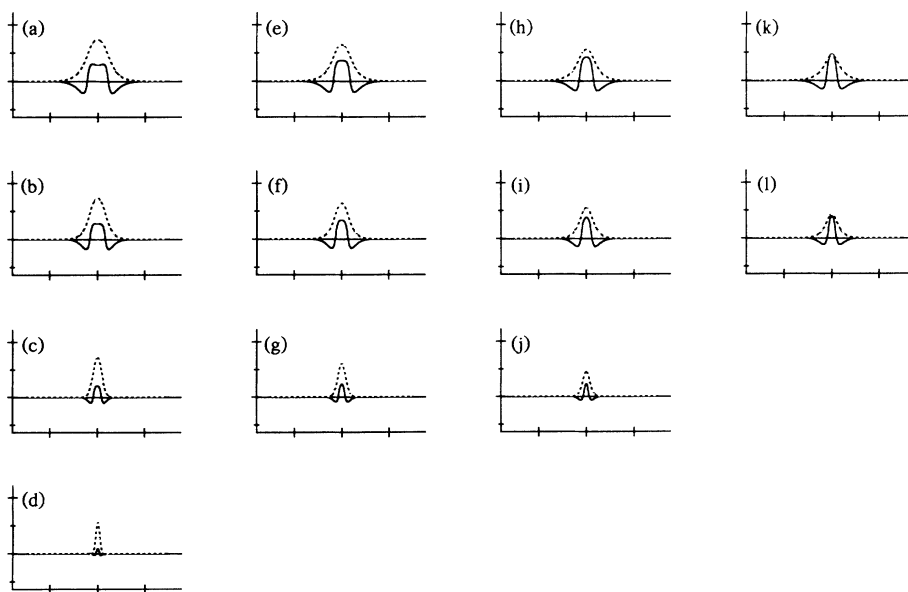Equation (3.13) has a solution if $1<D<9$. This corre-

FIG. 9. Profiles of the motionless localized domains for various values of a and D. The meanings of the lines are the same as those in Fig. 1.

TABLE I. The values of the domain width for the motionless domains in Fig. 9.

	$a = 0.036$	$a = 0.065$	$a = 0.1$	$a = 0.15$
$D = 10.0$	(a) $R = 4.291$	(e) $R = 3.395$	(h) $R = 2.722$	(k) $R = 2.043$
$D = 5.0$	(b) $R = 3.135$	(f) $R = 2.497$	(i) $R = 1.991$	(l) $R = 1.435$
$D = 1.0$	(c) $R = 1.608$	(g) $R = 1.226$	(j) $R = 0.8442$	
$D = 0.1$	(d) $R = 0.5280$			

sponds to the curves for intermediate values of D, such as $D = 1.0$ and 5.0 in Fig. 6. For instance, we obtain $z_1 \approx 5$ for $D = 5$ in the limit $c \rightarrow 0$. Although this value is smaller than the numerical result by a factor of $\frac{1}{2}$, Eq. (3.13) obtained by the large D expansion is in accord qualitatively with the behavior in Fig. 6.

IV. PROFILES OF MOTIONLESS LOCALIZED AND PULSE SOLUTIONS

In the previous sections we have evaluated motionless localized and pulse solutions of Eqs. (1.1). The velocity of pulse solutions is multivalued as a function of the parameter a as in Fig. 5. Following the result of Rinzel and Keller [15], however, we should regard these slower pulses as unstable solutions.

In this section we shall study profiles of pulse and motionless solutions in the stable branches by changing the diffusion constant D and the parameter a. First we determine the parameter regions where these two solutions exist. The stability diagram is shown in Fig. 7. The region left of the line 1 is the one for stable motionless localized domains. The boundary line 1 is obtained from Fig. 3 by taking the maximum value a_c for each value of D. The area left of the line 2 is the region for stable pulse solutions. The line 2 is determined from Fig. 5. In the FitzHugh-Nagumo limit $D \rightarrow 0$, a pulse solution can exist up to the critical value a_{FN}. Notice that these two lines (1 and 2) cross each other at a_{cross}. Therefore the parameter space is divided into four subspaces, as is indicated by I, II, III, and IV in Fig. 7.

In region I, any stable nonuniform solution does not exist. In region II, the system has only a motionless solution. As the parameter a is decreased below a_{FN}, a stable pulse solution appears in region III. It is important to note that both motionless and pulse solutions can exist in region IV. The allowed interval of D for this coexistence becomes wider by decreasing a.

Now we compare the spatial profiles of the solutions at various points in the a-D space. Figure 9 shows the profiles of the motionless localized solutions. The parameters for each figure are indicated by the crosses in Fig. 8. The signs associated with Fig. 9 correspond to those in Fig. 8. We have chosen other parameters as $\epsilon = \beta = 1$ and $\gamma = 0$. The values D and a and the half-width R of these profiles are given in Table I.

It is found from Fig. 9 that a motionless domain becomes narrower as D decreases or as a increases. However, the mechanisms are quite different. When we increase a, the rest state becomes more stable so that the excited region shrinks. On the other hand, when we decrease D, the inhibitor does not spread so that it suppresses the ac-

tivator more efficiently and the width of the profile of u as well as the height becomes small.

Next let us discuss the pulse solutions for the parameters indicated by the crosses in Fig. 10. Figure 11 shows their profiles where we have dropped the solutions at (n), (o), (p), (r), and (s) because of the reason mentioned at the end of this section. The velocity c and the width z_1 for each solution are given in Table II, where we have chosen the solutions with higher speed. One can see that as a increases, the pulse becomes smaller. This tendency is similar to that of motionless solutions. Notice that the pulse width becomes wider when we decrease D for a fixed value of a. This is opposite to the case of motionless solutions.

The above property can be understood as follows. When D is 0.0001 and 0.1, profiles of the pulse are not so different from each other as can be seen from Figs. 5 and 6. On the other hand, in the case of large D, the inhibitor diffuses rapidly and affects the front of the pulse so that the pulse width has to be smaller. When D becomes still larger, a pulse solution is unable to exist since the inhibitor which spreads by diffusion suppresses completely the growth of u at the pulse front $z = z_1$.

In this way we can understand the D dependence of the pulse profile qualitatively. To summarize, if D is very small, a pulse propagates stably with larger height and high velocity, whereas if D becomes large, its existence is unfavorable. As a result we see that diffusion of the inhibitor plays an opposite role for the stability of a motionless solution and a solitary pulse solution.

For comparison, we have plotted the motionless and the pulse solutions for the same parameters in Figs. 9 and 11. Especially, (b), (c), and (d) in Fig. 9 and (m) in Fig. 11 are the solutions for $a = 0.036$. Thus one can see how the
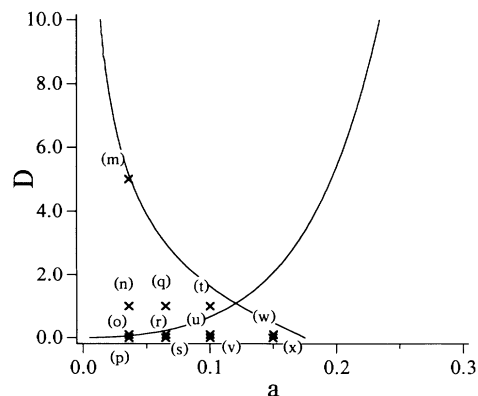

FIG. 10. The values of a and D for propagating pulses shown in Fig. 11.
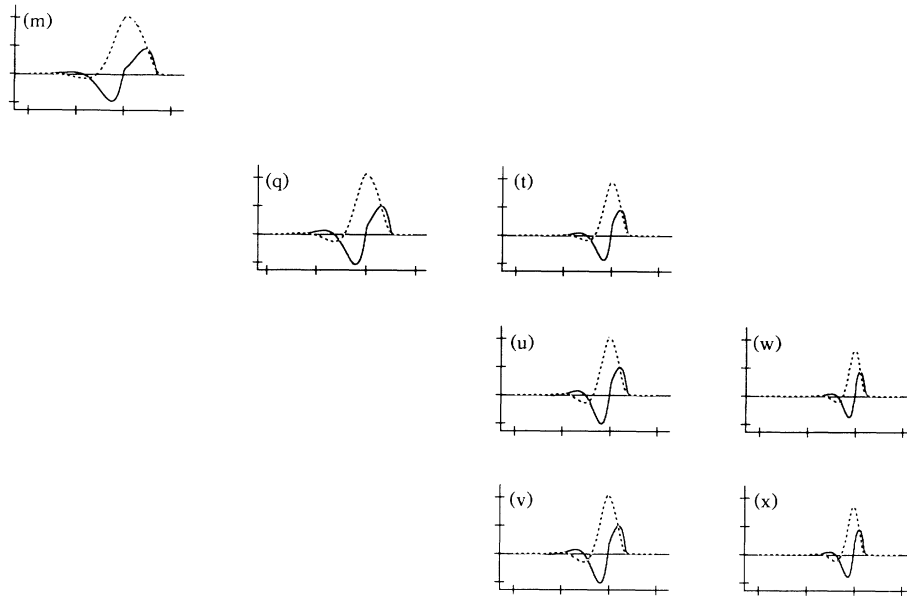
FIG. 11. Profiles of the solitary pulse solutions for various values of a and D. The meanings of the lines are the same as those in Fig. 4.

profiles change in the coexistence region depending on the diffusion constant.

An isolated propagating pulse is expected to be unstable for the parameters indicated by (n), (o), (p), (r), and (s) in Fig. 10. Note that a pulse has a tail where the value of u becomes positive. If the maximum of u at the tail region is larger than a, the activator is expected to grow, so that a pulse is unstable. This situation violates the condition (3.6) for pulse width since it assumes that u exceeds a only at two points $z = 0$ and z_1. What actually happens is an emergence of traveling wave trains [15]. This is indeed the case for the parameters (n), (o), (p), (r), and (s).

V. DISCUSSIONS

We have shown that depending on the magnitude D of the diffusion constant of the inhibitor, there are two localized solutions in the excitable reaction-diffusion equation (1.1). One is a propagating pulse which appears for small values of D. The other is a motionless localized solution for large values of D. Although each of these solutions had been studied in detail previously, the crossover from one to the other changing the diffusion constant has not been investigated. One of our main conclusions in this paper is that these two solutions can coexist in some parameter regime.

It is remarked here that although we have dealt with only motionless localized and propagating pulse solutions, the behavior of the system in the crossover region is actually more complicated. Not only an isolated pulse but also bound states of propagating pulses are expected to exist. We have some evidence for this by computer simulations of (1.1) [16].

In part II of this series of papers, we have shown that in-phase and antiphase breathing motions can exist in periodic excited domains described by (1.1). This together with the present results about the coexistence of different types of dynamical solutions leads us to a notion

TABLE II. The values of the pulse width and the speed for the pulse solutions in Fig. 11.

	$a \approx 0.036$	$a \approx 0.065$	$a \approx 0.1$	$a \approx 0.15$
$D = 5.0$	(m) $a = 0.03600$ $z_1 = 13.89$ $c = 3.87$			
$D = 1.0$		(q) $a = 0.06490$ $z_1 = 10.50$ $c = 3.42$	(t) $a = 0.10019$ $z_1 = 6.563$ $c = 2.37$	
$D = 0.1$			(u) $a = 0.10019$ $z_1 = 7.052$ $c = 2.56$	(w) $a = 0.15013$ $z_1 = 3.785$ $c = 1.68$
$D = 0.0001$			(v) $a = 0.10015$ $z_1 = 7.082$ $c = 2.57$	(x) $a = 0.14976$ $z_1 = 3.918$ $c = 1.72$

of *dynamical bistability* [17]. In thermodynamic equilibrium where a system is variational, bistability is a basic concept to understand phase transitions and phase equilibria. In a nonvariational system far from equilibrium, on the other hand, various types of active order or pattern can emerge as a stationary state, which may coexist. A transition from one active state to another would also be possible by, e.g., external disturbance or noise. Although this type of dynamical bistability seems not to have been observed experimentally so far, it is our belief that interplay between different active states has an important implication for self-organization in biological systems.

ACKNOWLEDGMENTS

APPENDIX

We derive the pulse solution of the BvP equation, i.e., u_c and v_c, in the moving coordinate $z = x - ct$. Equation (1.1) with Eq. (1.2) can be written in terms of u_c and v_c as

$$-c\epsilon\tau\frac{du_c}{dz} = \epsilon^2\frac{d^2u_c}{dz^2} - u_c + \Theta(u_c) - v_c , \qquad \text{(A1a)}$$

$$-c\frac{dv_c}{dz} = \epsilon D\frac{d^2v_c}{dz^2} + \beta u_c - \gamma v_c . \qquad \text{(A1b)}$$

Eliminating u_c, we obtain the following differential equation of v_c:

$$\epsilon^3 D\frac{d^4v_c}{dz^4} + \epsilon^2 c(\tau D + 1)\frac{d^3v_c}{dz^3} + \epsilon(\tau c^2 - \epsilon\gamma - D)\frac{d^2v_c}{dz^2}$$
$$- c(\epsilon\gamma\tau + 1)\frac{dv_c}{dz} + (\beta + \gamma)v_c - \beta\Theta(z)\Theta(-z + z_1) = 0 . \qquad \text{(A2)}$$

Here we have assumed that the excited region is confined to the interval $0 < z < z_1$. Equation (A2) is linear in v_c so that u_c and v_c are expressed as a linear combination of the exponentials $\exp(\alpha_i z)$, respectively, for both the excited and the rest domains. Here α_i $(i = 1,2,3,4)$ are roots of the equation $P(\alpha) = 0$ given by Eq. (3.3). Equation (3.3) with $c = 0$ reduces to the characteristic equation (2.2) for a motionless localized solution.

The coefficients of the exponentials in Eq. (3.2) are determined by the boundary conditions at $z = \pm\infty$, i.e.,

$$u_c(\pm\infty) = v_c(\pm\infty) = 0 \qquad \text{(A3)}$$

and the matching conditions such that u_c and v_c and

their first derivatives are continuous at the interface, i.e.,

$$u_c(+0) = u_c(-0), \quad u_c(z_1 + 0) = u_c(z_1 - 0) , \qquad \text{(A4a)}$$

$$v_c(+0) = v_c(-0), \quad v_c(z_1 + 0) = v_c(z_1 - 0) , \qquad \text{(A4b)}$$

$$\left.\frac{du_c}{dz}\right|_{+0} = \left.\frac{du_c}{dz}\right|_{-0}, \quad \left.\frac{du_c}{dz}\right|_{z_1+0} = \left.\frac{du_c}{dz}\right|_{z_1-0} , \qquad \text{(A4c)}$$

$$\left.\frac{dv_c}{dz}\right|_{+0} = \left.\frac{dv_c}{dz}\right|_{-0}, \quad \left.\frac{dv_c}{dz}\right|_{z_1+0} = \left.\frac{dv_c}{dz}\right|_{z_1-0} . \qquad \text{(A4d)}$$

Rinzel and Keller [15] utilized the jump condition for second derivatives of u when they solved the FitzHugh-Nagumo equation. It is readily found that the matching condition of first derivative of the inhibitor v is equivalent to it.

After straightforward but very tedious calculation, we obtain the pulse solution of the BvP equation as (3.2) where the coefficients are given by

$$A_{11} = \frac{h(\alpha_1)}{\alpha_1 P'(\alpha_1)}(1 - e^{-\alpha_1 z_1}) , \qquad \text{(A5a)}$$

$$A_{12} = \frac{h(\alpha_2)}{\alpha_2 P'(\alpha_2)}(1 - e^{-\alpha_2 z_1}) , \qquad \text{(A5b)}$$

$$A_{21} = -\frac{h(\alpha_1)}{\alpha_1(P'(\alpha_1)}e^{-\alpha_1 z_1} , \qquad \text{(A5c)}$$

$$A_{22} = -\frac{h(\alpha_2)}{\alpha_2 P'(\alpha_2)}e^{-\alpha_2 z_1} , \qquad \text{(A5d)}$$

$$A_{23} = -\frac{h(\alpha_3)}{\alpha_3 P'(\alpha_3)} , \qquad \text{(A5e)}$$

$$A_{24} = -\frac{h(\alpha_4)}{\alpha_4 P'(\alpha_4)} , \qquad \text{(A5f)}$$

$$A_{33} = \frac{h(\alpha_3)}{\alpha_3 P'(\alpha_3)}(e^{-\alpha_3 z_1} - 1) , \qquad \text{(A5g)}$$

$$A_{34} = \frac{h(\alpha_4)}{\alpha_4 P'(\alpha_4)}(e^{-\alpha_4 z_1} - 1) , \qquad \text{(A5h)}$$

$$B_{ij} = -\frac{\beta}{h(\alpha_j)}A_{ij} , \qquad \text{(A6)}$$

with

$$i = 1,2,3, \quad j = 1,2,3,4, \quad h(\alpha) = \epsilon D\alpha^2 + c\alpha - \gamma ,$$

$$P'(\alpha) = \frac{dP(\alpha)}{d\alpha} .$$

We have verified that Eq. (3.2) with these coefficients agrees with that obtained by Rinzel and Keller [15] in the limit $D = \gamma = 0$.

[1] S. Koga and Y. Kuramoto, Prog. Theor. Phys. **63**, 106 (1980).

[2] T. Ohta, R. Kobayashi, and M. Mimura, Physica D **34**, 115 (1989).

[3] O. Thual and S. Fauve, J. Phys. **49**, 1829 (1988).

[4] A. Joets and R. Ribotta, Phys. Rev. Lett. **60**, 2164 (1988).

[5] K. Toko, M. Nosaka, T. Fujiyoshi, K. Yamafuji, and K. Ogata, Bull. Math. Biol. **50**, 225 (1988).

[6] H. G. Purwins, Ch. Radehaus, T. Dirksmeyer, R. Doh-
    men, R. Schmeling, and H. Willebrand, Phys. Lett. A **136**,
    480 (1989) and the earlier references cited therein.

[7] Q. Quyang and H. L. Swinney, Nature (London) **352**, 610
    (1991).

[8] U. Rau, K. M. Mayer, J. Parisi, J. Peinke, W. Clauss, and
    R. P. Huebener, Solid-State Electron. **32**, 1365 (1989).

[9] T. Ohta, A. Ito and A. Tetsuka, Phys. Rev. A **42**, 3225
    (1990).

[10] T. Ohta and H. Nakazawa, Phys. Rev. A **45**, 5504 (1992).

[11] H. P. McKean, Adv. Math. **4**, 209 (1979).

[12] P. C. Fife, SIAM (Soc. Ind. Appl. Math.)-AMS (Am.
     Math. Soc.) Proc. **10**, 23 (1976).

[13] R. FitzHugh, Biophys. J. **1**, 445 (1961); J. Nagumo, S. Ari-
     moto, and S. Yoshizawa, Proc. IRE **50**, 2061 (1962).

[14] M. Mimura (unpublished).

[15] J. Rinzel and J. B. Keller, Biophys. J **13**, 1313 (1973).

[16] R. Kobayashi, A. Ito, and T. Ohta (unpublished).

[17] The concept of dynamical bistability has been introduced
     in a slightly different context by Mikhailov *et al.* See Ch.
     Zulicke, A. S. Mikhailov, and L. Schimansky-Geier, Phy-
     sica A **163**, 559 (1990).